

Hydrogenated silicon carbon nitride films obtained by HWCVD, PA-HWCVD and PECVD techniques

I. Ferreira ^{a,*}, E. Fortunato ^a, P. Vilarinho ^b, A.S. Viana ^c, A.R. Ramos ^d,
E. Alves ^d, R. Martins ^a

^a CENIMAT, Departamento de Ciência dos Materiais da Faculdade de Ciências e Tecnologia da UNL and CEMOP-UNINOVA
Campus da FCT-UNL, 2829-516 Caparica, Portugal

^b CICECO, Departamento de Engenharia Cerâmica e do Vidro da Universidade de Aveiro, 3810-193 Aveiro, Portugal

^c ICAT, laboratório de SPM da Faculdade de Ciências, Universidade de Lisboa, Campo Grande, 1749-016 Lisboa, Portugal

^d ITN, Instituto Tecnológico e Nuclear, Estrada Nacional 10, 2686-953 Sacavém, Portugal

Available online 17 April 2006

Abstract

Hydrogenated silicon carbon nitride (SiCN:H) thin film alloys were produced by hot wire (HWCVD), plasma assisted hot wire (PA-HWCVD) and plasma enhanced chemical vapor (PECVD) deposition techniques using a Ni buffer layer as catalyst for inducing crystallization. The silicon carbon nitride films were grown using C₂H₄, SiH₄ and NH₃ gas mixtures and a deposition temperature of 300 °C. Prior to the deposition of the SiCN:H film a hydrogen etching of 10 min was performed in order to etch the catalyst material and to facilitate the crystallization. We report the influence of each deposition process on compositional, structural and morphological properties of the films. Scanning Electron Microscope-SEM and Atomic Force Measurement-AFM images show their morphology; the chemical composition was obtained by Rutherford Backscattering Spectrometry-RBS, Elastic Recoil Detection-ERD and the structure by Infrared-IR analysis. The thickness of the catalyst material determines the growth process and whether or not islands form. The production of micro-structured SiCN:H films is also dependent on the gas pressure, gas mixture and deposition process used.

© 2006 Elsevier B.V. All rights reserved.

PACS: 81.05.Gc; 73.61.Jc; 81.15.-z

Keywords: Amorphous semiconductors; Composition; Films and coatings; FTIR measurements; Nitrogen-containing glass

1. Introduction

The exceptional mechanical, tribological and optical properties of ternary SiCN thin film alloys make them suitable for a wide range of applications. Profiting of the wide band gap controllability between 5 eV, for SiN, and 2.8 eV, for SiC [1], SiCN films can be used in optoelectronic applications such UV detection [2,3] or low-voltage white-blue electroluminescence devices [4]. Due to its low dielectric constant k , below 5, SiCN films have been successfully applied in the protection of metal interconnection of ultra

large-scale integrated circuit (ULSI) [5] as etch stop and hardmask. Crystalline SiCN films were employed in high breakdown-voltage heterojunction diodes for high-temperature [6]. Applications of SiCN to MEMS have been also reported [7] making use of its exceptional mechanical properties like high hardness in the range of SiC and SiN materials ≈ 30 GPa [1]. Adding together a good chemical resistance make this ternary alloy particularly interesting for tribological applications.

Several processes were used to produce amorphous or crystalline SiCN thin films alloys. Amorphous SiCN films are produced frequently by PECVD-like techniques using substrate temperatures below 600 °C, while crystalline SiCN films reported have principal deposition process

* Corresponding author. Tel.: +351 21 294 8564; fax: +351 21 295 7810.
E-mail address: imf@fct.unl.pt (I. Ferreira).

based on CVD techniques for substrate temperatures above 800 °C.

A large variety of alloys $\text{Si}_x\text{C}_y\text{N}_z$ can be obtained depending on the gas mixture and on carbon and nitrogen sources. Extra alloying elements such oxygen and hydrogen are of great importance and a source of complication for understanding its role on the main mechanical, optical structural and electrical properties.

In this paper we compare the structure, morphology and composition of SiCN:H films produced by HWCVD assisted or not by rf plasma and compared it to the films obtained by PECVD technique. This leads to the production of SiCN:H crystalline films by PA-HWCVD without incorporation of oxygen.

2. Experimental

The $\text{Si}_x\text{N}_y\text{C}_z\text{:H}$ films were produced by hot wire chemical vapor deposition (HWCVD), plasma assisted HWCVD (PA-HWCVD) and plasma enhanced chemical vapor deposition (PECVD) using a gas mixture of silane (SiH_4), ethylene (C_2H_4) and ammonia (NH_3) without hydrogen dilution. For the HWCVD process the filament temperature was kept at 1900 °C while for the PECVD component an rf power of 130 W was applied. A gas mixture consisting of $\text{SiH}_4/\text{C}_2\text{H}_4/\text{NH}_3$ was fed into the reactor in the proportion of 10/50/200 sccm, respectively. The system employed was described in a previous work [8]. The films were deposited on normal glass and crystalline silicon (c-Si) substrates and on thin (50 or 100 Å) Ni covered layer c-Si high resistivity wafer and glass substrates. The films composition was analyzed by RBS and by ERD. He-RBS spectra were obtained with 2 Schottky barrier detectors placed in IBM geometry at 140° and 180° scattering angles, with resolutions of 15 and 20 keV respectively, using 2.0 MeV He^+ beam. ERD spectra were obtained with a Schottky barrier detector placed at 24° scattering angle in IBM geometry, with 20 keV resolution, using a 2.0 MeV He^+ beam. To prevent backscattered He^+ particles from hitting the ERD detector, a Kapton filter with 8.2×10^{19} at/cm² was placed in front of it. IR absorption spectra were acquired with FTIR equipment in the wavenumber range of 400–4000 cm^{-1} . SEM images were taken with a Hitachi-S400 apparatus on films covered with a very thin carbon conductive layer. Tapping mode AFM experiments were performed in a Multimode AFM microscope coupled to a Nanoscope IIIa Controller. Commercial etched silicon tips with typical resonance frequency of a.c. 300 Hz, have been used as AFM probes.

3. Results

The FTIR spectra obtained for HWCVD, PA-HWCVD and PECVD films are shown in Fig. 1. The main assigned vibrations are related to: N–H ($\approx 3300 \text{ cm}^{-1}$), C–H ($\approx 2800 \text{ cm}^{-1}$) and C–N ($\approx 2100\text{--}2150 \text{ cm}^{-1}$) stretching modes; N–H₂ wagging modes ($\approx 1500 \text{ cm}^{-1}$); Si–N (stretch-

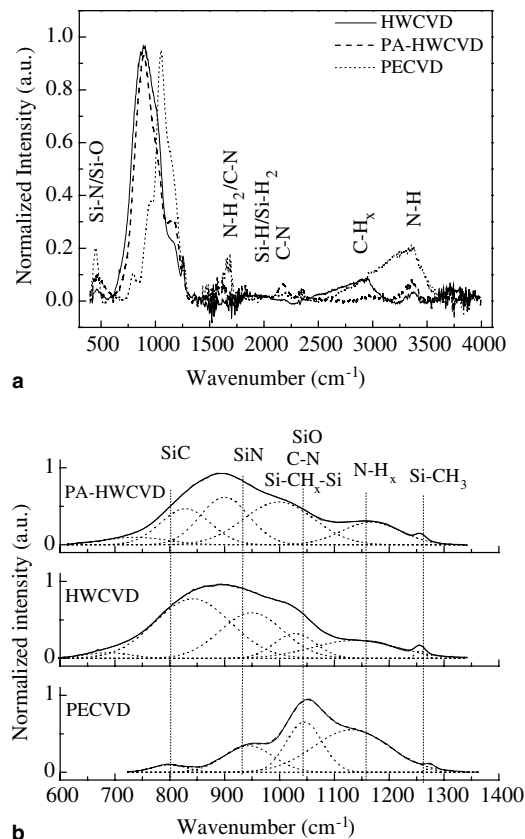


Fig. 1. (a) FTIR spectra of SiCN films produced by different processes, HWCVD, PA-HWCVD and PECVD; (b) expansion of the same spectra in the wavenumber range of 600–1400 cm^{-1} . Dashed lines represent the deconvoluted peaks.

ing)/Si–O (rocking) modes ($\approx 450 \text{ cm}^{-1}$); and a strong absorption band in the wavelength range of 600–1300 cm^{-1} , due to SiC, SiN, SiO, Si–CH_x, C–N vibration modes [5,9,10]. An enlargement and deconvolution of the spectra in this region was performed in order to obtain the relative intensity, position and area of each peak. That is shown in Fig. 1(b) and summarized in Table 1.

Although similar deposition parameters were used for the films production, IR data show that the process rules the species incorporated into the film and therefore its composition. The main difference between the three process employed is related to the incorporation of C and N. On HWCVD films C and N is preferentially bonded to silicon atoms due to the fact that SiC and SiN peaks are the most intense. Significant N–H_x bonds are also present both revealed by the N–H_x bending and stretching bonds. Since no peak related to C–N stretching modes is observed, we relate the peaks at 1000–1030 cm^{-1} to the presence of SiO or Si–CH_x–Si bonds. On the other hand, PECVD films show less C bonded to Si (weak SiC peak), an important amount of N is bonded to Si but major C and N are bonded in the hydroxyl groups (Si–CH_x–Si; N–H_x, C–H). For PA-HWCVD films an intermediate situation, as far as composition is concerned, is achieved. Still a high amount of C and N bonded to Si but inferior to that one

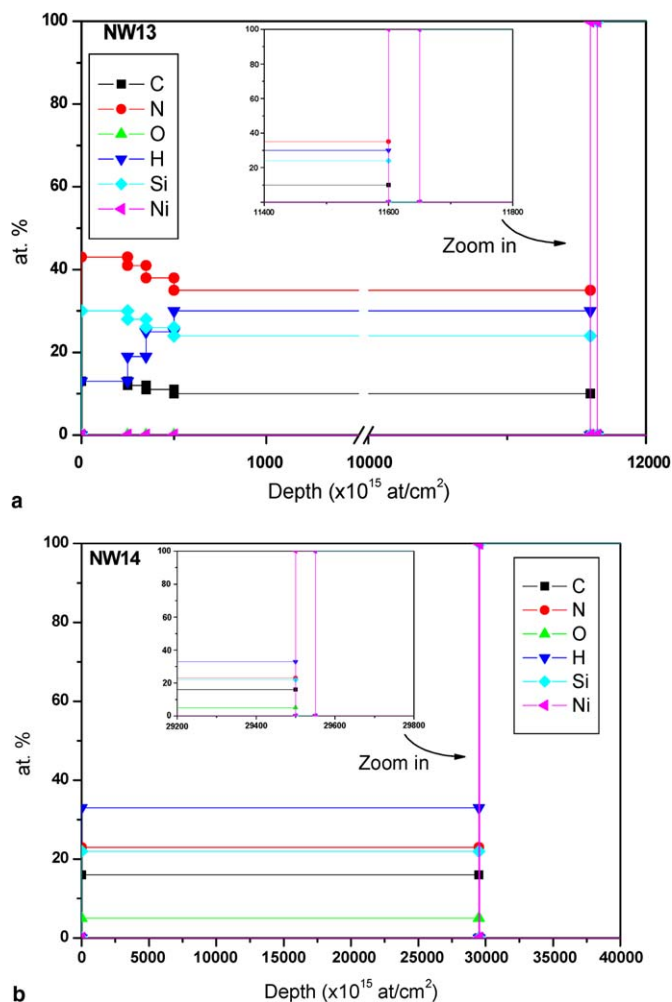


Fig. 2. Depth profile obtained from RBS and ERD spectra for samples produced by (a) PA-HWCVD; and (b) HWCVD. The inset displays a magnification of the region where Ni is present.

shown by HWCVD films appears and the Si–H and SiO/C–N/Si–CH_x–Si peaks are enhanced when compared to both HWCVD and PECVD films.

The FTIR measurements were supplemented by RBS and ERD analysis shown in Fig. 2.

Fig. 2 shows the depth profile obtained for the elements detected by RBS and ERD analyses, after data simulation, of the samples produced by PA-HWCVD (Fig. 2(a)) and HWCVD (Fig. 2(b)). The average percentage of elements detected is shown in Table 2.

Under similar deposition conditions used for the films production we get Si_{0.24}C_{0.11}N_{0.35}H_{0.30} and Si_{0.22}C_{0.16}N_{0.23}O_{0.05}H_{0.33} for PA-HWCVD and HWCVD films, respectively. So far, HWCVD films have more carbon incorporation and lower nitrogen content but some porosity is revealed by the presence of oxygen in contrast to the PA-HWCVD films. On the other hand, results also reveal a thin Ni layer at the glass interface. That layer corresponds to the 5 nm Ni layer used as catalyst for inducing crystallization. The inset of the graphs in Fig. 2(a) and (b) evidence a 5 nm layer corresponding to the thickness of the deposited Ni layer. Therefore we conclude that Ni was not consumed during the deposition process.

Not only is the composition influenced by the deposition process, but also the film morphology is quite different. Fig. 3 shows the SEM cross section images of the PECVD (Fig. 3(a)), PA-HWCVD (Fig. 3(b)), and HWCVD (Fig. 3(c)) films deposited on Ni 5 nm covered glass and c-Si substrates. The films of Fig. 3(a) are compact, have low surface roughness and are amorphous while Fig. 3(b) exhibit compact films but with high surface roughness formed by isles with variable dimensions that are independent of the substrate used, glass or Si-c, if covered with thin Ni layer. SEM images of Fig. 3(c) shows films, deposited on Si + Ni 5 nm substrate, that are compact, structured and crystalline with a cone-like surface. When deposited on glass, the films are amorphous with a smooth surface.

The real dimensions of the isles are supported by AFM data that is exhibited in Fig. 4, for PA-HWCVD films. There a 3D profile image is shown in Fig. 4(a) and the section analysis across the line displayed is shown in Fig. 4(b).

Table 1

Summary data of the peak position, area and respective modes obtained for HWP, PA-HWCVD and PECVD films whose IR spectra are shown in Fig. 1(b)

Peak position (cm ⁻¹)	Modes	Relative area		
		HWP	PA-HWCVD	PECVD
≈690–710	Si–H rocking and wagging	8	14	–
≈830–832	SiC stretching and wagging	133	53	7.9
≈900–940	SiN stretching	85	69	39
≈1000–1030	SiO (stretching)/C–N (wagging)/Si–CH _x –Si (bending)	30	88	53
≈1130–1160	N–H _x (bending)	44	40	95
≈1250	Si–CH ₃ (bending)	2.2	1.7	0.9

Table 2

Results of the composition obtained by RBS and ERD for PA-HWCVD and HWCVD films

Sample	C at. %	N at. %	O at. %	H at. %	Si at. %	Thickness ×10 ¹⁵ at/cm ²
PA-HWCVD	11	35	0	30	24	11 600
HWCVD	16	23	5	33	22	29 500

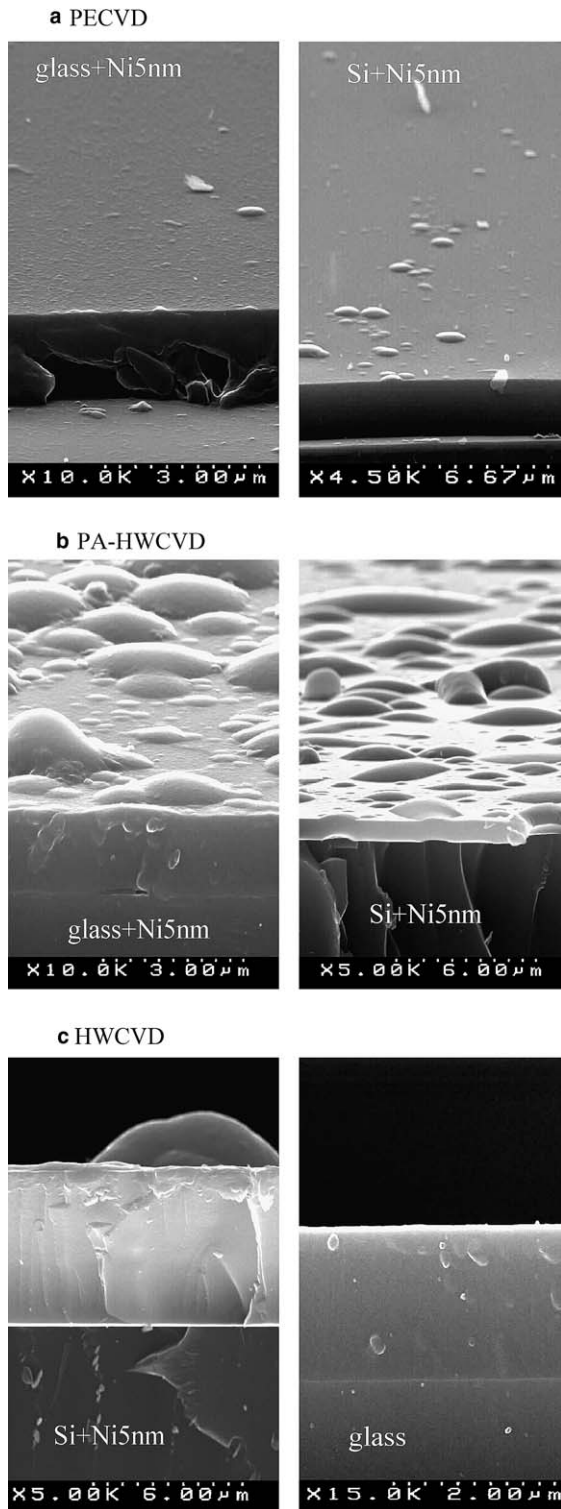


Fig. 3. SEM cross section view images of (a) PECVD film deposited on Ni (5 nm) covered glass and on Ni (5 nm) covered Si-c substrates; (b) PA-HWCVD film deposited on Ni (5 nm) covered glass and on Ni (5 nm) covered Si-c substrates; (c) HWCVD film deposited on Ni (5 nm) covered Si-c and on glass substrates.

We observe that isles are cone-like shape and their dimensions are variable from few nanometers to several microns. The big one observed in the image of Fig. 4(b) is about

2.5 μm in diameter and around 200 nm in height. Also we have observed that the surface morphology is dependent on the Ni thickness as shown in Fig. 5. Fig. 5(a) shows the SEM top view images of a SiCN film deposited on Ni (1 nm) covered Si-c substrate. Fig. 5(b) and (c) shows the image of the same film deposited on Ni (5 nm) and Ni (10 nm) covered glass, respectively, obtained in sample region absent of isle. Surface morphology is dependent on Ni thickness, some grains appear to be involved by the amorphous tissue in Si-c substrate covered with a Ni 1 nm layer, while in glass substrates with Ni 5 nm and 10 nm layer we observed agglomerates that are smoother than the former.

4. Discussion

The comparison process (keeping the same deposition parameters) evidenced that HWCVD lead to a high incorporation into the SiCN films, of SiC and SiN bonds. As the rf plasma is coupled to HWCVD process the C and N starts to be incorporated in hydroxyl groups. Therefore for films grown by the PECVD the carbon and nitrogen are predominantly bonded to hydroxyl groups (Si-CH_x-Si; N-H, C-H). This difference in the films composition is attributed to the gas dissociation occurring in each process. It is well accepted and demonstrated that in HWCVD process the species containing hydrogen are highly dissociated giving rise to ionized species like Si, C, C₂ or N [8]. Additionally, NH₃ has low dissociation energy compared to C₂H₄ and high reactivity with carbon enhancing the incorporation of C_xN_y species and so it is responsible for increasing carbon content. This explains why SiC films (produced without ammonia gas) have a very low growth rate (~ 0.6 Å/s [8]) compared to the 5–6 Å/s obtained for these SiCN:H films. Besides that, CH_x species have also an etching effect on the film growth, and so its contribution to this growth mechanism cannot be disregarded. Although with FTIR measurements we cannot conclude about the presence of a SiCN ternary compound, it reveals that SiC and SiN bonds are the basis bonds for films deposited by HWCVD and PA-HWCVD techniques. PECVD films seem to be formed by different separated phase, since C-N, N-H and Si-CH_x-Si bonds are predominant, suggesting that a ternary alloy is not obtained.

SEM images have revealed that Ni is crucial for inducing crystallization since without that we observe a compact, smooth and featureless film. When a thin Ni buffer layer is used a high roughness surface is obtained, independently of Si-c or glass substrate used. The origin of these isles is unknown but certainly related to catalyst effect of Ni on the inducing crystallization which has to be confirmed by micro X-ray diffraction investigation in further work. For HWCVD films produced on (Si + Ni 5 nm) substrate it is quite evident the presence of a crystalline material being obtained a laminated like surface in the region of the layer break. The isle shown, in the SEM image, is also compact with a diameter of the order of 6 μm and height around

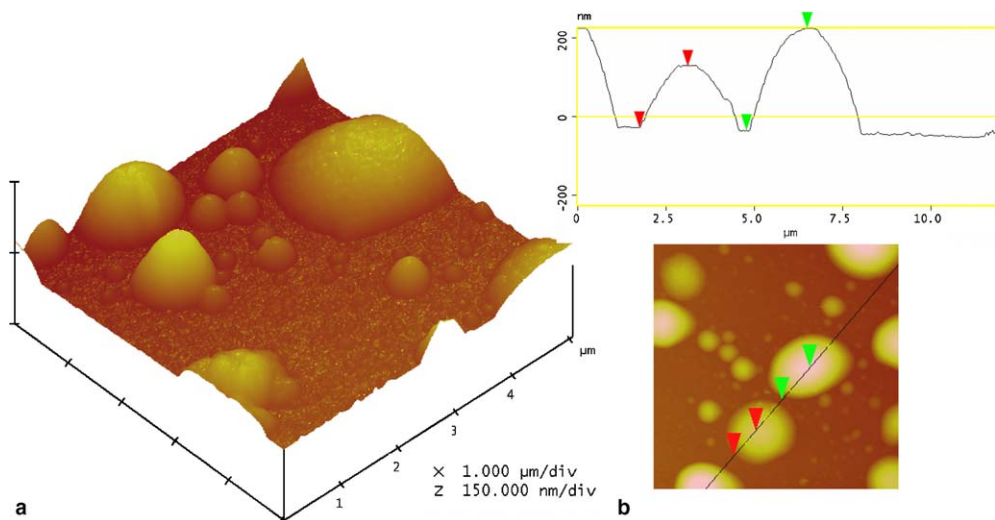


Fig. 4. AFM image of a SiCN PA-HWCVD film deposited on Ni (5 nm) covered glass: (a) 3D profile obtained in a $5 \mu\text{m} \times 5 \mu\text{m}$ scanned area and data scale of 150 nm; (b) profile obtained in a scanned area of $12.5 \mu\text{m} \times 12.5 \mu\text{m}$ with the respective section.

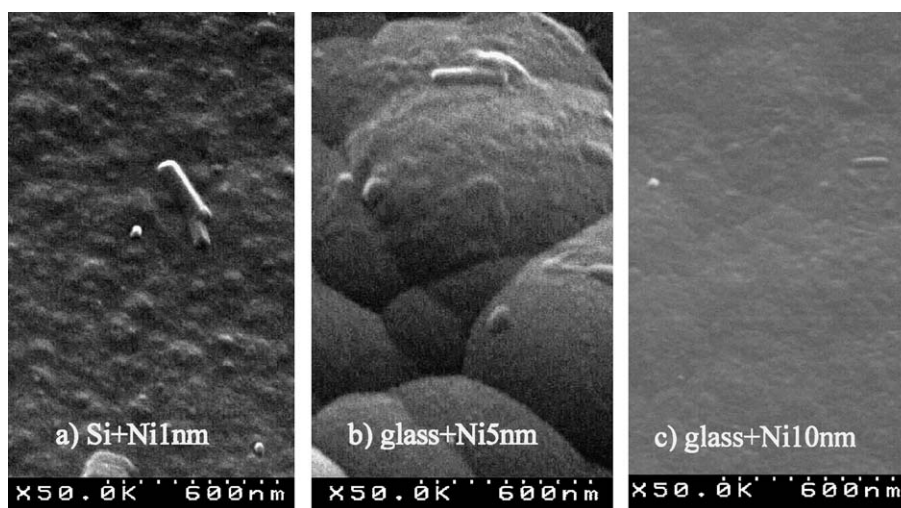


Fig. 5. SEM top view (with a tilt angle of 35°) images of a SiCN PA-HWCVD film deposited on: (a) Ni (1 nm) Si-c covered substrate; (b) Ni (5 nm) glass covered substrate; and (c) Ni (10 nm) glass covered substrate.

$2.4 \mu\text{m}$. The formation of this isle-like features in SiCN films was also reported by Gang et al. [11], being dependent on the N/H_2 ratio used, in films produced by bias-assisted HFCVD. Also Pandey et al. [12] found this clusters regions in diamond like carbon obtained by microwave plasma CVD, attributing that to sp^2 rich clusters, that have large surface roughness. In our case further investigations are needed to find the structure and composition of these cone-like regions. Nevertheless, Ni is certainly the origin of that, since the films deposited directly in Si-c or glass substrate did not exhibit those features.

On the other hand RBS also has indicated that Ni is not consumed during the deposition. The Ni buffer layer remains with a thickness around 5 nm for all films analyzed, which corresponds to the initial thickness. However, the Ni buffer layer is important for inducing crystallization and for the films morphology.

5. Conclusions

The study of the influence of the deposition process on the production of SiCN films, under similar deposition parameters led to the conclusion that HWCVD films have higher carbon incorporation with Si-C and Si-N making up the main bonds formed. PA-HWCVD films are N rich with the nitrogen not only bonded to silicon but also to carbon and hydrogen (C-N and N-H bonds are enhanced compared to HW-CVD films). PECVD films have C and N bonded preferentially in the hydroxyl groups and the main achieved bonds are those related to C-H, C-N and Si- CH_x -Si.

Concerning the morphology HWCVD and PA-HWCVD films exhibit an island-like surface with dimensions varying from a few nanometers up to about $6 \mu\text{m}$ in diameter and $3 \mu\text{m}$ in height, while PECVD films are

compact and have a smooth surface. The surface morphology features are due to the Ni buffer layer which, depending on its thickness in the range of 1 and 5 nm, gives rise to clusters whose composition will be investigated in further work.

Acknowledgements

This work was supported by ‘Fundação para a Ciência e Tecnologia’ (Foundation for Science and Technology) through a contract with CENIMAT and by the projects POCTI/CTM/38924/2001, POCTI/CTM/37344/2001, POSI-6207-AdI, and ASSEMIC network project MRTN-CT-2003–504826.

References

- [1] P. Jedrzejowski, J. Cizek, A. Amassian, J.E. Klemberg-Sapieha, J. Vlcek, L. Martim, *Thin Solid Films* 447&448 (2004) 201.
- [2] C.W. Chen, C.C. Huang, Y.Y. Lin, L.C. Chen, K.H. Chen, W.F. Su, *Diamond Relat. Mater.* 14 (2005) 1010.
- [3] W.-R. Chang, Y.-K. Fang, S.-F. Ting, Y.-S. Tsair, C.-N. Chnag, C.-Y. Lin, S.-F. Chen, *IEEE Electron Dev. Lett.* 24 (9) (2003) 565.
- [4] R. Reyes, C. Legnani, P.M. Ribeiro Pinto, M. Cremona, P.J.G. De Araújo, C.A. Achete, *Appl. Phys. Lett.* 82 (23) (2003).
- [5] Y.H. Wang, M.R. Moitreyee, R. Kumar, L. Shen, K.Y. Zeng, J.W. Chai, J.S. Pan, *Thin Solid Films* 460 (2004) 211.
- [6] S.-T. Ting, Y.-K. Fang, W.-T. Hsieh, Y.-S. Tsair, C.-N. Chang, C.-S. Lin, M.-C. Hsieh, H.-C. Chiang, J.-J. Ho, *IEEE Electron Dev. Lett.* 23 (3) (2002) 142.
- [7] Y. Liu, L.-A. Liew, R. Luo, L. An, M.L. Dunn, V.M. Bright, J.W. Daily, R. Raj, *Sensors Actuators A* 95 (2002) 143.
- [8] I. Ferreira, V. Silva, H. Águas, E. Fortunato, R. Martins, *Appl. Sur. Sci.* 184 (2001) 60.
- [9] J.-Y. Wu, C.-T. Kuo, P.-J. Yang, *Mater. Chem. Phys.* 72 (2001) 245.
- [10] E. Xie, Z. Ma, H. Lin, Z. Zhang, D. He, *Opt. Mater.* 23 (2003) 151.
- [11] Z. Gang, E.G. Wang, G.C. Xu, Y. Chen, *Thin Solid Films* 348 (1999) 114.
- [12] M. Pandey, D. Bhattacharyya, D.S. Patil, K. Ramachandran, N. Venkatramani, *Surf. Coat. Technol.* 182 (2004) 24.